

REMOTE SENSING FOR AnnAGNPS TO DEVELOP A METHOD OF CROP TYPE IDENTIFICATION WITH MULTI-TEMPORAL LANDSAT

James Coss, University of Toledo, Geography and Planning, james.coss@utoledo.edu

Kevin Czajkowski, University of Toledo, Geography and Planning

kevin.czajkowski@utoledo.edu

Ling Yao Michigan State, Geography, ling_yao_919@yahoo.com

Abstract Models used to predict soil loss and sediment constituency require a timely and spatially complete characterization of the region being modeled. For a model like AnnAGNPS data requirements extend beyond a simple land use and land cover data set to crop type. AnnAGNPS incorporates agricultural characterizations to include crop rotation and tillage practices. Generally, this information does not exist in the public record in the format necessary for the AnnAGNPS model. Digital image processing of remotely sensed imagery offers a resource that provides the timely and spatially complete data source from which to synthesize the information necessary to run the model. In particular, Landsat imagery provides the repetitive and synoptic imagery at a scale that fits very well the needs of the AnnAGNPS model. Multi-temporal/multi-spectral image processing provided accurate crop species mapping for this study. This method relies on the seasonal variation patterns of specific crops, including soybeans, corn and winter wheat, by identifying the unique observable spectral changes throughout the year. The technique was tested in the Sandusky watershed in Ohio in 2003 and 2004. Two problems with using the multi-temporal satellite images were identified including having a sufficient number of ground data points and just having enough images throughout the year. Several images used in the study had clouds and haze and various methods of atmospheric correction were used to increase the number of available images. Developing a list of known ground control points has required the use of Farm Service Administration aerial slides and manual image analysis. Once extracted these data were used to train and assess the accuracy of the crop rotation derived from the Landsat imagery. Finally, total accuracy of crop type was greater than 85 percent for both years.

Introduction

There has been growing interest in linking the preservation of water quality to agricultural land practices in the Sandusky River watershed. A number of simulation models have been developed to evaluate water quality parameters affected by agricultural land management at both field scale and watershed scale (Zhou, 1997). The most widely used models include CREAMS (Chemicals, Runoff, Erosion for Agricultural Management Systems), EPIC (Erosion-Productivity Impact Calculator), AGNPS (Agricultural Non-Point Source Pollution Model), and SWAT (Soil and Water Assessment Tool), which is part of BASINS (Better Assessment Science Integrating Point and Non-point Sources) developed by the U.S. EPA. These models have been used to predict various impacts of land management on water quality (e.g., Srinivasan and Aronod 1994, Muttiah and Wurbs 2002), sediment yield and nutrient loss (e.g., Luzio et al., 2002), and pesticide fate and transport (e.g., Brown and Hollis 1996) in a wide range of watershed scales from a few dozen hectares to thousands of square kilometers (Wu et al., 2003). Among many agricultural practices considered in these models, crop rotation is regarded as a basic but important practice that has significant influences on water quality.

To date there is no comprehensive inventory of crop types on the basis of each farm field for the Sandusky River watershed, which directly resulted in no complete crop rotation information over the entire watershed. Currently, crop type data is collected for only 10% of the farm fields every year by the USDA through ground surveying due to the high cost of human labor involved in driving and inspecting each field (Farmer Service Agency, 2004). The crop rotation information is necessary in order to fully understand the quantitative relationships between farming practices and water quality in the Sandusky watershed. Thus, mapping crop types in continuous years for the watershed has become a necessity.

The Sandusky River is the second largest river draining into Lake Erie in the State of Ohio, with a drainage area of 1,421 square miles (Figure 1). The Sandusky River watershed is an agriculture-dominated area, with 84% of the land used for crop production (Ohio Department of Agriculture, 1995). Over the last decades as the population grew, the use of agricultural chemicals became widespread and the number of livestock increased, the water quality of the river has declined, resulting in loss of biodiversity and health impacts from contaminated water. There has been growing interest in linking the preservation of water quality to agricultural land practices in the Sandusky River watershed. A number of simulation models have been developed to evaluate water quality parameters affected by agricultural land management at both field scale and watershed scale (Zhou, 1997).



Figure 1. Sandusky drainage basin.

METHODOLOGY

Sensor Preparation Landsat 5, which was launched in 1984, carries the 30-meter Thematic Mapper (TM) scanner. The TM scanner provides seven multi-spectral channels (3 visible, 1 near-infrared, 2 mid-infrared, 1 thermal-infrared) at 30-meter resolution except for thermal-infrared at 120-meter resolution (NASA, 2005).

Multi-temporal remote sensing has had success in detecting the seasonal characteristics unique to each of the target species and has allowed the differentiation of crop types (Schriever et al., 1993). It takes into account changes in reflectance as a function of plant phenology (stage of growth) (Figure 1). Imagery from different times in the growing cycle can capture the unique phenology characteristics of each crop type and thus can be used to identify different crops otherwise difficult to distinguish (Figure 2).

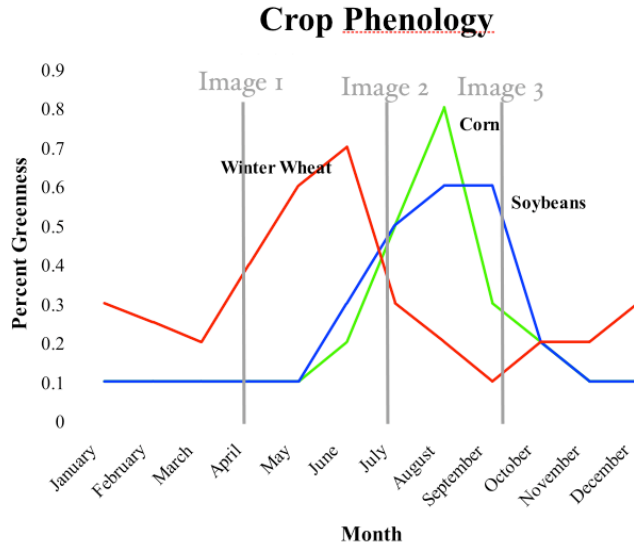


Figure 2. Spectral variation observed in vegetation throughout a year.

	2003	2004
Row 19 Path 31	04 /14 ◆◆◆ 09 /13 ◆◆◆ 10 /15 ◆◆◆ 12 /02 ◆◆◆	04/24 ◆ 06/27 ◆◆ 09/15 ◆◆◆ 10/01 ◆
Row 19 Path 32	04 /14 ◆◆◆ 09 /13 ◆◆◆ 10 /15 ◆◆◆ 12 /02 ◆◆◆	04/24 ◆ 06/27 ◆◆ 09/15 ◆◆◆ 10/01 ◆
	◆◆◆ Clear	◆◆ Cumulus cloud present ◆ Cirrus cloud present

Table 1. Landsat Imagery (2003 – 2004) Used in the Study.

The study area is covered by two scenes of Landsat ETM+ and TM imagery: path 19, row 31 and path 19, row 32. Landsat ETM+ imagery for these two scenes from 2003 and 2004 were examined and selected according to the extent of cloud cover. Cloud-free images were the most desirable. Because of the lack of cloud-free images in some years, some imagery with cumulus or cirrus clouds was also considered usable, but these images required further processing to get rid of the cloud before they could be used in the classification. Some Landsat TM imagery from 2003 were also used in this study because ETM+ data on Landsat 7 satellite developed the Scan Line Corrector (SLC) anomaly.

This research is focusing on agricultural areas of the watershed and therefore non-agricultural regions were such as urban and quarry were masked out.

Atmospheric Correction Fair weather cumulus is a cloud type that frequently appears in satellite images. Cumulus clouds not only “block” the land cover below them from the sensor, they also reflect solar radiation away, casting shadows on the ground. This shadowing effect reduces solar radiation at the surface. The true reflectance of the land cover under the cumulus cloud and the spots where the shadow is cast is thus unknown from the imagery. The influence of the cumulus cloud and its shadow appears to be significant and there is no way to recover the lost information.

The methods that we used to mask the cumulus cloud and the shadow are in fact quite simple. First, thresholds on the band ratio of Landsat band one and band six (band1/band6) were used to distinguish cloud pixels from other pixels (Jackson, 2004). Compared to pixels of cloud-free land cover, pixels of cumulus clouds usually have higher values in band 1 and lower values in band 6, which makes their ratios of band1/band6 have much larger values than those of other pixels. Pixels of shadows were identified by using thresholds respectively on band 1, band 2, band 3 and band 4 (Jackson, 2004). These thresholds were developed for each image through a heuristic approach. A binary mask was built after the identification of the cloud and shadow pixels. The mask has the same dimension as the original image. The pixels in the mask that correspond to the cloud and shadow pixels had value 0, while all other pixels in the mask had the value 1. Then, by applying a binary mask derived from the previous process, value 0 was assigned to the cloud and shadow pixels and values of other pixels stayed unchanged.

Training Data For soybean, wheat, corn, hay/pasture and their subclasses, we acquired training information from either the ground surveying conducted in 2004 by James Coss. For 2003, we acquired the ground truth information for the crop types from the true-color aerial photos that we purchased from Farmer Service Agencies (FSA) of four counties in Ohio including Wyandot, Crawford, Sandusky and Seneca. Each photo is 1024 x 1536 pixels, with a ground resolution of approximately 3 meters (10 feet) (Figure 3). The aerial photographs were scanned at the resolution of 2400 dots per square inch (dpi). Each scanned image was then identified in the flight line map, oriented north, and named according to the county, the year, the flight line number and the slide number. Because the scanned images were recorded in the coordinates of the scanner, they needed to be converted to reflect their position in the real world so that the crop type information is tied with the correct farm field. This was accomplished by using georeference tools in ArcGIS to line up the aerial photographs with a projected street layer. After georeferencing, the aerial photos were ready for interpretation.



Figure 3. Aerial photo used in the training set.

An interpretation key was developed after carefully reviewing the four photographic characteristics of different crop types including corn, soybean, hay, and winter wheat. An interpretation key is a set of guidelines used to assist interpreters in identifying features (Reising, 2005). Winter wheat was the easiest crop to distinguish due to its unique yellowish/brownish tone because almost all winter wheat were headed by the time that the aerial photographs were taken. Corn and soybean can be differentiated from the tone and texture. Soybean usually has a lighter green tone and a smooth texture, while corn typically shows a darker green tone and a rough texture. The differences between corn and soybean can be very apparent in aerial photos taken in late July or early August when corn was silked and soybean was setting pods. However, in some photos acquired in late June and early July, the differences can sometimes be unnoticeable because both corn and soybean were just planted. Crop stress resulting from moisture problems, fertilizer problems, insect and disease problems, and weed and herbicide problems can also cause changes in tone, texture, pattern and shape and thus need to be considered in crop identification.

Classification A maximum likelihood classifier within ENVI was used on the multi-temporal Landsat imagery. There were a total of seven types of land use/land cover defined in the study, including soybean, wheat, corn, fallow, riparian, water, and forest. The crop type for a given year is defined as whatever crop was growing in the farm field on June 15th that year. This date was chosen because all major crops including winter wheat were usually growing on this date. Winter wheat planted in fall will not be counted as the crop for that year, i.e. the previous summer. Instead, it will be considered as the crop for next year. However, whether winter wheat was planted in the following fall does influence the classification of the crop type for that year, because winter wheat has a very different spectral signature curve from that of a fallow field. For instance, if we use three Landsat images acquired separately in April, June, and October to classify corn, the corn fields with winter wheat growing in October will have different phenology pattern over the year compared to the corn fields with nothing growing in October.

For other classes including water, fallow, riparian areas, and forest, we developed the training points from Landsat images. They can be easily recognized in Landsat images due to their unique spectral signatures. Because water is a strong absorber of near infrared radiation, clear water usually appears much darker in band 4 (near-infrared) than vegetation and soil. The reflectance of turbid water is usually bigger than that of clean, clear water, but still usually smaller than vegetation and soil. That is why clean, clear water in forest area usually look darker

than water with industrial pollution in an industrial area or water with suspended soils in a flood plain.

Fallow fields are those that are not planted for a period of time so that they can regain their fertility. They usually appear from brown to tan in true-color Landsat composites. Mid-spring (April or May) images together with early-summer (June) images were used to identify training data for fallow fields for each year. If there was no crop growing in the field on both images, then the field was determined as fallow for that year.

Post Classification Three post-classification techniques were applied in this study to improve the classification results. We first used one of ENVI's post-classification functions, Sieve Classes to solve the problem of isolated pixels occurring in the classification images. Sieving classes removes isolated classified pixels using blob grouping (ENVI online manuals). Although low pass or other types of filtering techniques could also be used to remove these isolated pixels, the class information would be contaminated by adjacent class codes (ENVI online manuals). The sieving class method looks at the neighboring 4 or 8 pixels to determine if a pixel is grouped with pixels of the same class (ENVI online manuals). If the number of pixels in a class that are grouped is less than the value that you enter, those pixels will be removed from the class (ENVI online manuals). When pixels are removed from a class using sieving, black pixels (unclassified) will be left (ENVI online manuals).

Another post-classification procedure, Clump Class, was performed after the sieving class, in which adjacent similar classified areas will be clumped together using morphological operators (ENVI online manuals). Classified images often suffer from a lack of spatial coherency (speckle or holes in classified areas) (ENVI online manuals). Again, low pass filtering could be used to smooth out these in coherencies, but the class information would be contaminated by adjacent class codes. Clumping classes solves this problem (ENVI online manuals). The selected classes are clumped together using a kernel of the size specified in the parameters dialog (ENVI online manuals).

After the classified images were sieved and clumped, ENVI's Combine Classes function was used to combine two subclasses to one big class. For instance, the wheat-none subclass was combined with wheat-wheat subclass to one big wheat class. This wheat class includes both wheat pixels with wheat growing again in the fall and wheat pixels without anything planted in the fall.

ENVI's post-classification accuracy assessment tools were used to calculate a confusion matrix (contingency matrix) for each classification result using ground truth ROIs. The confusion matrix can show us the accuracy of a classification result by comparing the classification result with the ground truth information that we acquired from either ground surveying or aerial photographs. Over 150 points were prepared for each of the other classes using the ground truth information. For major crop classes, corn, soybean, and winter wheat, over 300 points were prepared. The exact same ground truth information was used to build the confusion matrices for the classification on both the MNF transformed imagery and non-MNF transformed multi-temporal Landsat imagery (Table 2 and Table 3)

Classes	Ground truth information (pixels)						
	Soybean	Corn	Wheat	Fallow	Forest/Riparian	Water	Total
Soybean	729	81	0	0	0	0	810
Corn	32	808	0	0	0	0	840
Wheat	76	0	636	48	0	0	760
Fallow	0	0	0	256	0	0	256
Forest/Riparian	59	0	0	0	486	0	545
Water	0	0	0	0	0	308	308
Unclassified	0	0	0	0	0	0	0/0
Total	896	889	636	304	486	308	3519

Table 2. 2003 Confusion matrices

Classes	Ground truth information (pixels)						
	Soybean	Corn	Wheat	Fallow	Forest/Riparian	Water	Total
Soybean	348	25	0	82	0	0	455
Corn	32	77	43	2	60	2	516
Wheat	0	0	432	0	0	0	432
Fallow	0	0	0	187	0	0	187
Forest/Riparian	0	87	0	0	324	1	417
Water	0	0	0	0	0	165	165
Unclassified	0	0	0	0	0	12	12
Total	380	489	475	271	384	180	2179

Table 3. 2004 Confusion matrices

CONCLUSION

The overall accuracy is an average with the accuracy of each class weighted by the proportion of test samples for that class in the total training or testing sets (Brandon R. Bottomley, 1998). A widely used, acceptable accuracy is 85%, which is striven for in the land use classification adopted by the U.S. Geological Survey (Brandon R. Bottomley, 1998). The accuracy assessment reports indicated that for the year 2004, the overall accuracy of the classification of multi-temporal Landsat imagery is 88.94%. For 2003, the overall accuracies were 93.55% for the classification of multi-temporal Landsat imagery. This means that close to or over 85% of all the pixels tested were correctly classified in the classifications according to the ground truth information.

The overall accuracies of the classifications were very close to or higher than the widely used standard of 85% for acceptable classifications. The values of kappa coefficients (over 80%) for all the classifications also indicated strong agreement between the classification results and the ground truth information. The values of these two indices, overall accuracy and the kappa efficient, together confirmed the general effectiveness of the methodology used in this thesis project for crop classification, especially the experimental cloud removing techniques and the tentative methods for extracting crop type information from aerial photographs (Figure 4).

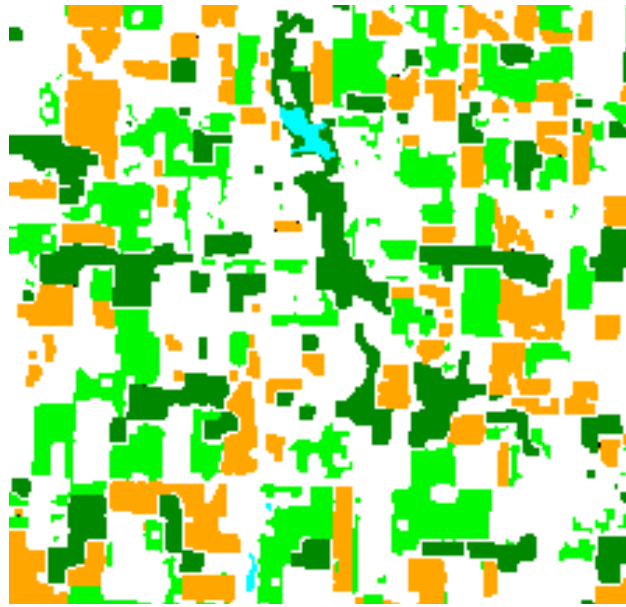


Figure 4. Results of crop mapping using multi-temporal remote sensing with Landsat 2004.

REFERENCES

- Brandon R. Bottomley. 1998. Mapping Rural Land Use & Land Cover Change In Carroll County, Arkansas Utilizing Multi-Temporal Landsat Thematic Mapper Satellite Imagery.
- Gregory, Megan. 2004. Conservation Farming Practices — a presentation prepared for the Cannon River Watershed Partnership. St. Olaf College, Environmental Studies.
- Jackson, Thomas, J. 2004. Procedure for Developing the Supervised Land-cover Classification Image for SGP99. <http://daac.gsfc.nasa.gov/fieldexp/SGP99/LC991shtml>.
- Luzio, M. D., R. Srinivasan, and J.G. Arnold. 2002. Integration of watershed tools and SWAT model into BASINS. *Journal of the American Water Resources Association* 38: 1127-1141.
- Muttiah, R. S., and R. A. Wurbs. 2002. Scale dependent soil and climate variability effects on watershed water balance of the SWAT model. *Journal of Hydrology* 256: 264-285.
- Schriever, J.R., and R.G. Congalton, 1993. Mapping Forest Cover-Types in New Hampshire Using Multi-Temporal Landsat Thematic Mapper Data. *ASPRS/ACSM Annual Convention & Exposition*, 15 – 19 February (New Orleans, Louisiana), Vol. 3. p. 333-342.
- Srinivasan, R., and J. G. Arnold. 1994. Integration of a basin-scale water quality model with GIS. *Water Resources Bulletin* 30: 453-462.
- Zhou, Yan and Chris Fulcher. A Watershed Management Tool Using SWAT and ARC/INFO. *Proceedings: The 17th Annual Environmental Systems Research Institute Users Conference*, San Diego, CA, July 8-11, 1997.